neutral dimer is quite strongly bound compared to iron, $D°(Nb_2)$ = 5.2 eV, making formation of large neutral fragments possible.

The relative bond strengths of niobium and iron clusters may reflect fundamental differences in the bonding of these two metals. Nb–Nb bonds are much stronger than Fe–Fe bonds, and it seems reasonable to attribute this to multiple metal–metal bonds for Nb. Since Fe is on the right-hand side of the periodic table, its 3d orbitals are contracted compared to those of Nb. Consequently, Fe_n^+ cluster bonding is thought to have less d–d interaction and proportionately more 4s–4s bonding.[42,43]

Another possible reason for the difference in fragmentation patterns between these two metals is that Nb and Fe clusters have different structures. For instance, a linear chain of atoms might be expected to break apart into molecular fragments upon collision, producing ionic and neutral cluster moieties. In contrast, a nearly close-packed structure may prefer to dissociate by popping-off random atoms sequentially from the cluster. Unfortunately, there is no structural information available on Fe or Nb clusters, although isomers of Nb_n have been previously postulated to account for apparent two-component reaction rates for niobium clusters.[44,45]

In this study, Nb_n^+ with even numbers of atoms are found to be more stable than Nb_n^+ with odd numbers of atoms (Table II). The CID branching ratios of the clusters generally reflect these relative binding energies. At higher energies, where extensive fragmentation occurs, product ions with even numbers of atoms consistently have higher relative probabilities for formation. These branching ratios are especially evident in comparison of Nb_5^+ and Nb_6^+ CID (Figure 1, d and e). If we take the primary CID product (Nb_{n-1}^+) as a standard, the secondary product (Nb_{n-2}^+) is relatively favorable in CID of Nb_6^+, where the secondary product is Nb_4^+, than for CID of Nb_5^+ to form Nb_3^+. Similarly, the tertiary product (Nb_{n-3}^+) is relatively favored in Nb_5^+ CID, where the product is Nb_2^+, compared to Nb_6^+ where the tertiary product is Nb_3^+. The same branching ratio effect can be seen for the quaternary products.

V. Conclusions

We have shown that ion beam studies can provide a wealth of quantitative information on transition-metal clusters. In this work, both ionic and neutral binding energies are derived from CID cross section threshold analysis. These BDEs, in turn, yield the cluster ionization potentials. In these systems, the numerous CID product channels provide redundant and complementary information, such that a consistent set of thermochemical data is obtained. The qualitative cross section energy dependences and the relative energy thresholds furnish insight into the mechanisms of Nb cluster dissociation.

In the future, we plan to extend this study to larger Nb_n^+, which will also provide information on the neutral clusters, since the IPs of larger clusters are already known.[37] Because the IPs of these large clusters do not decrease monotonically, it will be interesting to see if the same fragmentation pattern is observed. Determination of quantitative information though is not limited to CID processes, but through application of these techniques to reactive systems, we expect to gain thermochemical, kinetic, and mechanistic information on chemical reactions of metal clusters. We anticipate that niobium clusters should be very interesting reactive species, because of the strong bonds that can be formed with other molecules and atoms and the strong bonds within the clusters themselves.

Acknowledgment. This work is supported by the Army Research Office, DAAL03-87-2211.

Registry No. Nb_2^+, 73145-87-6; Nb_3^+, 99775-01-6; Nb_4^+, 73145-88-7; Nb_5^+, 73145-89-8; Nb_6^+, 73145-90-1; Nb, 7440-03-1; Xe, 7440-63-3.

(42) Shim, I.; Gingerich, K. A. *J. Chem. Phys.* **1982**, *77*, 2490.
(43) Leopold, D. G.; Almlof, J.; Lineberger, W. C.; Taylor, P. R. *J. Chem. Phys.* **1988**, *88*, 3780.
(44) Hamrick, Y.; Taylor, S.; Lemire, G. W.; Fu, Z.-W.; Shiu, J.-C.; Morse, M. D. *J. Chem. Phys.* **1988**, *88*, 4095.
(45) Zakin, M. R.; Brickman, R. O.; Cox, D. M.; Kaldor, A. *J. Chem. Phys.* **1986**, *88*, 3555.

Orientational Analysis of Micelle-Associated Trehalose Using an NMR–Pseudoenergy Approach

Preetha Ram, L. Mazzola, and J. H. Prestegard*

Contribution from the Chemistry Department, Yale University, New Haven, Connecticut 06511.
Received July 15, 1988

Abstract: A combined NMR–pseudoenergy approach to conformational and orientational analysis is applied to trehalose, a disaccharide with known membrane surface associative properties. Trehalose is incorporated into a medium composed of discoidal cesium perfluorooctanoate micelles that order spontaneously in high magnetic fields, and NMR data in the form of deuterium quadrupole splittings and dipolar splittings for carbon–proton and proton–proton interactions are acquired in suitably deuterated molecules. Preferred orientations of trehalose relative to micellar surfaces are initially sought by searching for director axes that approximately satisfy all the experimental observations. The director orientation and molecular conformations are then optimized by a modified molecular mechanics program in which orientational information from both deuterium quadrupole splittings and dipolar splittings is represented by pseudoenergy terms added to the program's empirical description of molecular energies. By this approach it has been possible to find probable conformations and orientations for trehalose on the micellar surface.

Carbohydrates perform a variety of functions at the surface of biological membranes.[1] As glycoconjugates of lipids and proteins, they act as receptors for a number of hormones and toxins; they also contribute significantly to the structural integrity of membranes. As simple saccharides they participate in a number of metabolic functions and even aid in protection from severe environmental fluctuations. The disaccharide trehalose, for example, is believed to aid in protection of cell membranes from the effects of dehydration and freezing by extensive hydrogen bonding to the phospholipid headgroups.[2,3]

(1) Sharon, N.; Lis, H. *Mol. Cell. Biochem.* **1982**, *42*, 167–187.
(2) Crowe, J. H.; Crowe, L. M.; Carpenter, J. F.; Rudolph, A. S.; Wistrom, C. A.; Spargo, B. J.; Anchordoguy, T. J. *Biochim. Biophys. Acta* **1988**, *947*, 367–384.

0002-7863/89/1511-3176$01.50/0

Despite the widely recognized importance of carbohydrates anchored or associated with membrane surfaces, there is little understanding of the physical basis of interfacial interaction. In an effort to improve this understanding, we began several years ago to develop methods for the study of orientational preferences of simple saccharides near membranelike interfaces.[4-6] This work exploited the orientational dependence of deuterium quadrupole splittings from deuterium-labeled carbohydrates in NMR spectra and employed magnetic field oriented micellar liquid crystals to provide well-ordered membranelike surfaces. While liquid-crystal micelles, consisting of aqueous dispersions of fatty acids, may have been an oversimplified model for actual cell membranes, they represented a preliminary step toward more complex systems. The liquid-crystalline medium we use here is closely related to the potassium laurate micelle system used previously and is composed of cesium perfluorooctanoate (CsPFO). This system offers some advantage over the potassium laurate micelles in that they are based on a more bilayer-like, disk-shaped micelle. The disks also orient with their normal axis parallel to the field and are stable near pH 7.[7]

Following previous work, we will continue to use deuterium quadrupole data on sugars deuterated by catalytic exchange in Raney nickel/deuterium oxide. This type of information has been successfully exploited in the study of lipids and glycolipids by a number of workers in the field.[8-12] Deuterium NMR has proved useful in structural analysis due to the existence of a quadrupole moment for the deuterium nucleus. As with any nucleus of spin $I > {}^1/_2$, deuterium posesses an asymmetrical charge distribution on the nucleus which allows it to interact with electric field gradients in addition to the static and radio frequency magnetic fields normally employed in NMR experiments. The quadrupole interaction perturbs the Zeeman energy levels ($m = -1, 0, 1$) producing nondegenerate $\Delta m = 1$ transitions. The splitting between these transitions, ν_q, is a function of nuclear properties, molecular geometry, and the degree of motional averaging in the system. It is generally assumed that all carbon–deuterium bonds have sufficiently similar electron distributions and nuclear quadrupole interactions to be described by a common coupling constant, $e^2qQ/h = 170$ kHz.[13] In liquid-crystal systems, splittings are related to this coupling constant by a term dependent on the angles of C–D bonds relative to the principal axes for an order tensor and a series of order parameters.[13] We will assume that motions in the liquid crystal are axially symmetric, so that their effects on doublet splittings can be described by a single-order parameter, S_z, involving a single director axis. For the CsPFO micelles, symmetry suggests this axis to be perpendicular to the micelle surface and parallel to the magnetic field. Geometric parameters are then confined to the angles, θ, that various C–D bond vectors have relative to the director in the molecular frame of the saccharide. The resulting equation for an observed quadrupole splitting is[13]

$$\Delta\nu = 3e^2qQ/2h\{(3\cos^2\theta - 1)/2\}S_z \qquad (1)$$

With the occurrence of several noncollinear C–D bonds it would, in principle, be possible to determine a unique orientation of the motional averaging axis relative to the molecular frame. Under ideal circumstances three such bonds would be sufficient, but due to the multivalued nature of the angular function and the fact that we cannot determine the sign of the splitting from the deuterium spectra, the number of bonds required to determine a unique orientation is often much greater. For trehalose, the number of independent C–D bond vectors is quite small. As can be seen in Figure 1, the most probable sites of ring deuterium exchange, are H2, H3, and H4, resulting in only two independent deuterium vectors. To improve orientational definition and provide some additional conformational information, we therefore will use dipolar interactions between carbons and their directly bonded protons, as well as between the pair of anomeric protons.

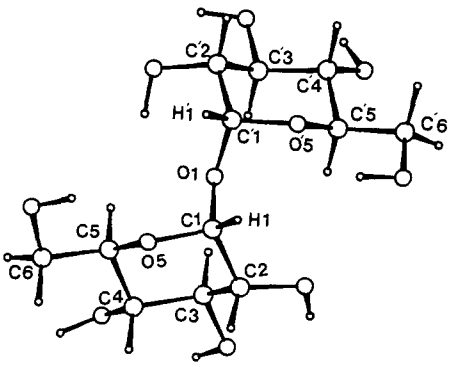

Figure 1. Structure of trehalose.

Dipolar coupling is a through-space interaction resulting from one nucleus coupling with the local magnetic field of a neighboring nucleus. These through-space interactions in isotropic fluids are averaged to zero by rapid isotropic tumbling, so dipolar coupling is normally not observed. However, just as orienting media restrict molecular tumblings and permit observation of quadrupolar doublets, dipolar couplings can be observed in field-ordered liquid-crystalline phases. Assumptions similar to those described above for motional averaging in the quadrupolar case lead to the following equation for the dipolar splitting observed for a pair of nonequivalent nuclei.[14]

$$\nu_d = \frac{\gamma_1\gamma_2 h(3\cos^2\theta - 1)}{2\pi r^3} \qquad (2)$$

Here γ_1 and γ_2 are the gyromagnetic ratios of the interacting nuclei separated by a distance r, and θ is the angle between the internuclear vector and director axis. For a ^{13}C–^1H pair directly bound to one another, r can be assumed fixed at 1.09 Å and the splitting used to provide angular information analogous to that from quadrupolar splittings.

A similar equation for the homonuclear case exists and only differs from eq 2 by a factor of 3/2. The distance between a pair of protons, r, also provides an internuclear distance as well as angular information. In the case of the anomeric protons in trehalose this is particularly useful, as their internuclear distance is a function of the glycosidic torsional angle. The combination of quadrupole coupling, ^{13}C–^1H dipolar coupling and ^1H–^1H dipolar coupling information should in principle allow determination of both orientational and conformational preferences.

Experimental Section

Due to the low gyromagnetic ratio and low natural abundance of the deuterium nucleus, proton for deuterium exchange is essential to the success of the proposed ^2H NMR experiments. It is also an important factor in reducing spectral complexity of ^{13}C and ^1H experiments. To accomplish deuteration we employed a Raney nickel catalyzed exchange reaction along the lines originally described by Koch and Stuart.[15] To improve efficiency and reduce side reactions the reaction mixture was sonicated and maintained at a lower temperature than usual.[16] Trehalose (0.3 g; Sigma, St. Louis, Mo.) was added to Raney nickel (2 mL settled volume) that had been purchased as a slurry from Aldrich,

(3) Lee, C. W. B.; Waugh, J. S.; Griffin, R. G. *Biochemistry* **1986**, *25*, 3737–3742.
(4) Prestegard, J. H.; Miner, V. W.; Tyrell, P. M. *Proc. Natl. Acad. Sci. U.S.A.* **1983**, *80*, 7192–7196.
(5) Tyrell, P. M.; Prestegard, J. H. *J. Am. Chem. Soc.* **1986**, *108*, 3990–3995.
(6) Miner, V. W.; Tyrell, P. M.; Prestegard, J. H. *J. Magn. Reson.* **1983**, *55*, 438–452.
(7) Boden, N.; Jackson, P. H.; McMullen, K.; Holmes, M. C. *Chem. Phys. Lett.* **1979**, *65*, 476–479.
(8) Griffin, R. G. *Methods Enzymol.* **1981**, *72*, 108.
(9) Seelig, J.; Macdonald, P. M. *Acc. Chem. Res.* **1988**, *20*, 221–228.
(10) Jarrel, H. C.; Jovall, P. A.; Giziewicz, J. B.; Turner, L. A.; Smith, I. C. P. *Biochemistry* **1987**, *26*, 1806–1811.
(11) Jarrel, H. C.; Wand, A. J.; Smith, I. C. P. *Biochim. Biophys. Acta* **1987**, *897*, 69–82.
(12) Skarjune, R.; Oldfield, E.; *Biochemistry* **1982**, *21*, 3154–3160.
(13) Abragam, A. *Principles of Nuclear Magnetism*; Clarendon Press: Oxford, 1961; pp 232–234.
(14) Harris, R. K. *Nuclear Magnetic Resonance Spectroscopy*; Pitman Books Ltd: London, 1983; pp 43–144.
(15) Koch, H. J.; Stuart, R. S. *Carbohydr. Res.* **1978**, *67*, 341–348.
(16) Cioffi, E. A.; Prestegard, J. H. *Tetrahedron Lett.* **1986**, *27*, 415–418.

preexchanged in 99.7% deuterium oxide, and added to 15 mL of D_2O. The mixture was heated to 80 °C and sonicated under argon for 10 h with approximately 40 W/cm² acoustic intensity at 20 KHz applied in a continuous mode through the titanium microtip of a Branson Model W-200P sonifier. At reaction termination the mixture was centrifuged, filtered through glass fiber, and passed through Chelex ion-exchange resin to remove remaining nickel impurities. Several samples were obtained at intervals during the reaction to monitor relative rates of deuterium incorporation by following the disappearance of signals in proton NMR spectra. Incorporation was pushed to approximately 80% exchange at the H2 and H4 sites of trehalose. Readily exchanged hydroxyl deuteriums were back-exchanged for protons when necessary.

The oriented liquid-crystal phase of cesium perfluorooctanoate (CsPFO) was prepared as described by Boden et al.[7] Cesium hydroxide was added to an aqueous solution of perfluorooctanoic acid until neutralized. The solution was dried and then resuspended as a 45% by weight dispersion in deuterium oxide solution for ^1H and ^{13}C spectra and distilled water for ^2H spectra. Trehalose was added to levels of 0.6–0.7 mol %, and the resulting sample was centrifuged in an NMR tube to effect mixing. To achieve orientation the sample was heated to 320 K in a 11.7-T field and slowly allowed to cool to an observation temperature of 308 K.

Carbon-13 and proton spectra were acquired with a Bruker WM500 spectrometer at operating frequencies of 125.7 and 500 MHz, respectively, acquiring 8 K time domain points in each case. Proton spectra were the result of 16 scans with a 90° pulse of 11 μs at a repetition rate of 2 s, using a sweep width of 2000 Hz. Carbon-13 spectra were collected by using an INEPT sequence so that signals from nonprotonated carbons (primarily those of the CsPFO) could be suppressed.[17] Typical spectra were the result of 4800 scans with a proton 90° pulse of 45 μs and a carbon 90° pulse of 9 μs. After an initial proton pulse, carbon–proton coupling was allowed to evolve for 3 ms and then magnetization sampled with a simultaneous proton and carbon 90° pulse. The relaxation delay was 2 s and the operating sweep width was 10 KHz.

Deuterium spectra were acquired on a home-built 11.5-T NMR spectrometer at a frequency of 75.2 MHz. A 90° pulse of 60 μs was employed for one-dimensional spectrum acquisition with a sweep width of 3000 Hz. Acquisition of deuterium two-dimensional multiple quantum (2D MQ) spectra employed a multiple-quantum NMR experiment described previously.[6] Double-quantum coherences were initiated by the first three pulses of the following pulse sequence: $(90\text{–}\tau/2\text{–}180\text{–}\tau/2\text{–}90\text{–}t_1\text{–}90\text{–}t_2)$. The period of $\tau/2$ is a nonincremented delay of 0.6 ms. The t_1 delay, initially of 50 μs, was incremented 32 times by 0.25 ms to complete a data set. The recycling time for each sequence was 0.2 s with a total acquisition time at each t_1 value of approximately 2 min. Phase cycling of the double-quantum pulses provides elimination of single-quantum signals and pulse artifacts. A second sequence with a 45° composite z rotation after double-quantum coherence was executed to allow quadrature detection in the t_1 dimension. The resulting data were transformed by the method of States[18] using a Gaussian weighting function in the t_1 and t_2 dimensions to produce a two-dimensional spectrum with t_1 and t_2 axes of double-quantum and single-quantum coherence, respectively.

Data were incorporated into a molecular modeling package AMBER,[19,20] and this package was used in searching for trehalose orientations and conformations that agreed with both experimental observations and theoretically allowed geometries. The details of data incorporation into the program are discussed later.

The conformational calculations were performed on a Vax 11/750 using the double-precision version of the AMBER energy minimization software. Both steepest descent and conjugate gradient minimization routines were used with the convergence criterion for the norm of the energy gradient set to be 0.5 kcal mol^{-1} Å^{-1}. Convergence to experimentally observed splittings was achieved on an average in less than 1 h of CPU time.

Results

Before orientational analysis could begin, it was necessary to determine the specific sites that had been deuterated by catalytic exchange of the trehalose molecule. Sites of deuteration were determined from comparison of a ^1H NMR spectrum of fully protonated trehalose to one at partial deuteration. The assignment

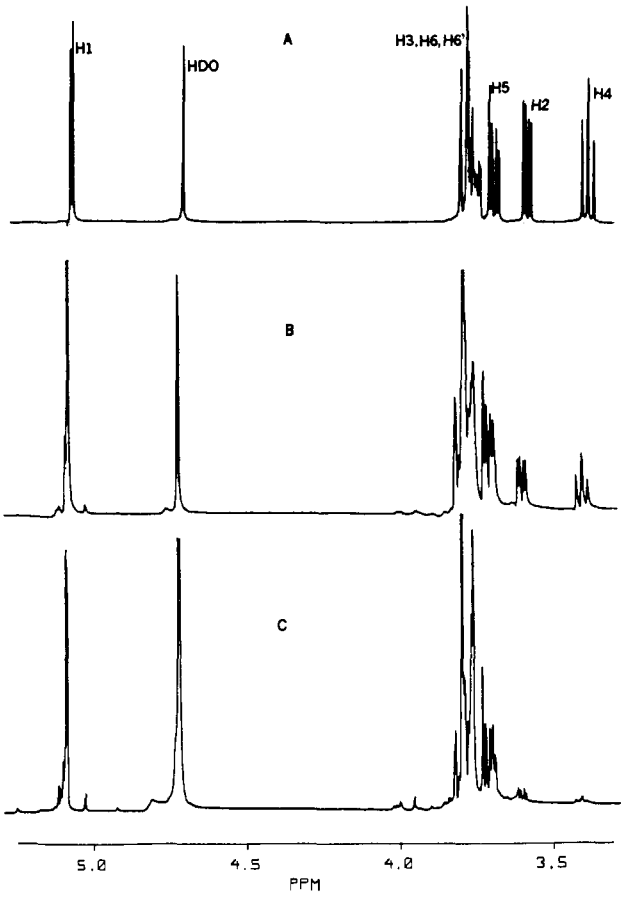

Figure 2. 500-MHz ^1H NMR spectrum of trehalose and deuterated trehalose in D_2O. (A) 0-h exchange, (B) 6-h exchange, (C) 10-h exchange.

of the fully protonated spectrum, as indicated in Figure 2, was based upon literature assignments.[21] All resonances are twofold degenerate because of the twofold axis of symmetry in the molecule. The extent of deuteration at each site was determined by integration of each resonance and comparison to the integral of the resonance for the anomeric proton which is known to be free of catalytic exchange. The disappearance of proton signals H2 and H4 as well as the collapse of the anomeric signal from a doublet to a singlet indicated that H2 and H4 had undergone nearly complete deuteration after 10 h. The remaining sites of deuteration are more difficult to assign due to spectral overlap. Integration of the H3–H6–H6′ region indicates a loss of approximately 1 proton. The possibility of H3 exchange can be ruled out by the retention of a doublet of doublet pattern for the H2 signal and the retention of a triplet pattern for the H4 signal at intermediate levels of deuteration. This suggests that intensity loss in this region is due to partial deuteration of H6 and H6′. This will be confirmed later by ^{13}C spectroscopy.

Acquisition of data on oriented molecules began with examination of deuterium spectra. The upper half of Figure 3 presents a deuterium spectrum of trehalose oriented in a CsPFO liquid crystal. The observed splittings cover a range of ~800 Hz. The two most intense peaks, with a splitting of 670 Hz, correspond to deuterium oxide present in the sample. Beyond this, the spectrum consists of four recognizable doublets. Since there are four sites on each ring, this suggests maintenance of an effective twofold symmetry axis in the liquid-crystal media. The noticeable difference in intensities of the lines corresponds directly to the extent of deuterium incorporation at each site and allows an assignment of the two most intense doublets to the H4 and H2 sites.

(17) Morris, G. A.; Freeman, R. *J. Am. Chem. Soc.* **1979**, *101*, 368.
(18) States, D. J.; Haberkorn, R. A.; Ruben, D. J. *J. Magn. Reson.* **1982**, *48*, 286–292.
(19) AMBER Copyright 1986, University of California, San Francisco, licensed from the Reagents of University of California.
(20) Weiner, S. J.; Kollman, P. A.; Nguyen, D. T.; Case, D. A. *J. Comput. Chem.* **1986**, *7*, 230–252.
(21) Bock, K.; Defaye, J.; Driguez, H.; Bar-Guilloux, E. *Eur. J. Biochem.* **1983**, *131*, 595–600.

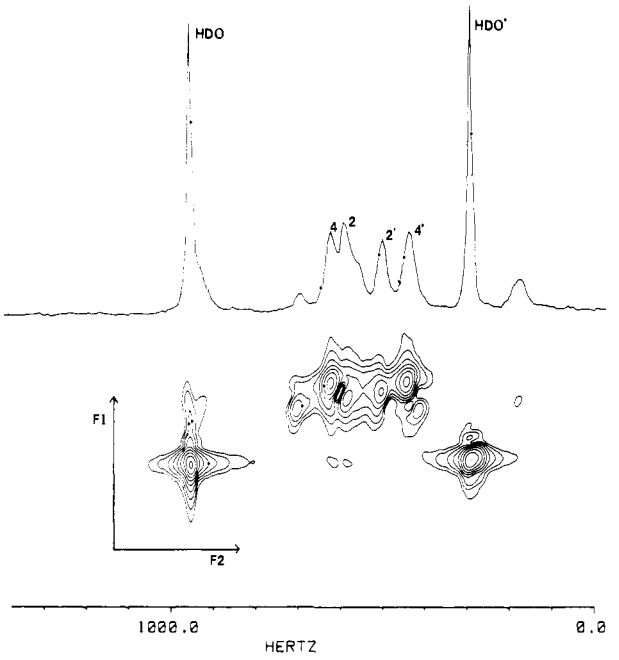

Figure 3. 75-MHz ^2H NMR spectrum of trehalose in CsPFO micelles.

Table I. Quadrupolar Splitting Data

^1H assignmt	splittings, Hz	^1H assignmt	splittings, Hz
HDO	670	H6[a]	282
H2	87	H6'[a]	730
H4	185		

[a] Tentative assignment.

More complete assignments can be made by comparison of chemical shifts for each doublet relative to its counterpart in the proton spectrum. Deuterium nuclei are subject to the same chemical shieldings as their hydrogen counterparts; consequently, the relative positions of signals at exchanged sites in the deuterium spectrum parallel those in the ^1H NMR spectrum. Chemical shift offset of deuterium spectra is unfortunately less than one-sixth the offset found in proton spectra. With the added complication of broader spectral lines due to the more efficient quadrupole relaxation mechanism, resolution of chemical shift in quadrupole spectra is often difficult. Deuterium double-quantum spectroscopy can be employed to separate chemical shift information from the quadrupole couplings, leading to less ambiguous pairing of resonances into doublets as well as chemical shift measurement. A two-dimensional multiple-quantum (2D MQ) NMR spectrum of deuterated trehalose in a liquid crystal is shown in the lower half of Figure 3. Chemical shift information alone is displayed in the F1 dimension, with chemical shift and quadrupole coupling information displayed in the F2 dimension. Based on chemical shift comparison, the most upfield doublet can be assigned to H4 and the most downfield to one of the H6 deuteriums. Splittings and proposed assignments are summarized in Table I.

The C2–H2 and C4–H4 bond vectors, which are quite rigidly oriented in the sugar rings, are most useful for geometrical analysis. Two facts about resonances from these sites should be noted. First, splittings are small relative to splittings observed previously in similar molecules.[5] Second, despite the fact that the C2–H2 and C4–H4 bond vectors are nearly collinear and should yield similar quadrupole splittings, the experimental values for the C2–H2 and C4–H4 splittings are significantly different. A narrow quadrupole splitting could, however, indicate the angle between the C–D bond vector and director axis to be near the magic angle, 54° (and correspondingly 126°). Slight deviations from this angle would produce large relative differences in quadrupole splitting values even for small deviations from collinearity. Under some circumstances it has been possible to use splittings assigned to C6–H6 bond vectors to characterize the geometry of the exocyclic hydroxymethyl group on hexopyranoses.[11] However, this requires

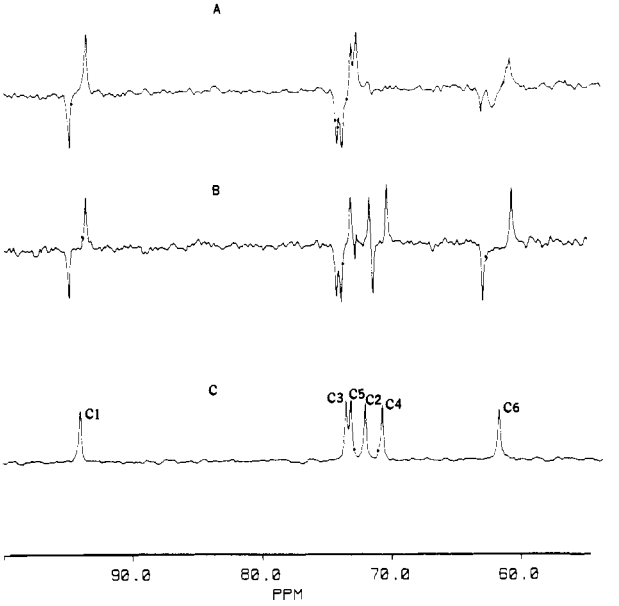

Figure 4. 125-MHz ^{13}C NMR spectrum of trehalose and deuterated trehalose in D_2O. (A) Deuterated trehalose, (B) fully protonated trehalose, (C) Fully protonated trehalose, decoupled.

both stereospecific assignment and observation of discrete conformational states of this rotationally labile group. Since we see no evidence of discrete states, we will not attempt to use the H6 or H6′ splittings.

^{13}C–^1H dipolar splittings, particularly for the anomeric site, provide some needed additional data. The dipolar splitting equation for a ^{13}C–^1H bond has the same functional dependence on the bond angle relative to the director axis as the C–D quadrupolar splitting. Analysis of ^{13}C–^1H dipolar spectra, however, poses two significant problems. The first arises from dipolar interaction within the molecule. Generally, every carbon in the glucose ring will interact with both directly bonded protons and nearby protons, producing a hopelessly complex spectrum. In this case, it is an advantage to have substantial deuteration at several adjacent sites. The C1–H1 bond vector benefits from the deuteration in that the second closest proton to C1, H2, has been exchanged for the low magnetic moment deuterium nucleus. The second problem arises from the liquid-crystal medium itself. The high concentration of perfluorooctanoic acid can produce a significant ^{13}C background signal. Carbons in CsPFO are, however, unique in that they are perfluorinated. This presents the possibility of using magnetization-transfer experiments that enhance signals of protonated ^{13}C carbons only. This requirement for a protonated carbon also aids in identification of deuterated sites. The INEPT pulse sequence (Insensitive Nuclei Enhanced by Polarization Transfer) is such an experiment.[17] Figure 4 compares ^{13}C NMR spectra of fully protonated trehalose, 4B, to deuterated trehalose in deuterium oxide, 4A, and decoupled trehalose, 4C. Assignments in the ^{13}C spectra were taken from literature references.[21,22] It is clear that signals from protonated carbons C3, C5, and C1 remain, along with signals from the proposed partially protonated carbons at C6.

The ^{13}C NMR INEPT experiment provides a unique opportunity to observe both J coupling (through bond) and dipolar coupling (through space) between the carbon and its bonded protons. In the nonoriented spectrum in Figure 4A, the splitting between the antiphase carbon peaks for the anomeric site (166 Hz) represents J coupling only, as the dipolar contribution is averaged to zero through isotropic tumbling. These splittings are independent of environment. A ^{13}C NMR INEPT spectrum of deuterated trehalose in a liquid crystal is shown in Figure 5 at two different temperatures. The C1 splittings in Figure 5 (46 Hz at 308 K) are sums of both J coupling and dipolar coupling. The

(22) Jeffrey, G. A.; Nanni, R. *Carbohydr. Res.* **1985**, *137*, 21–30.

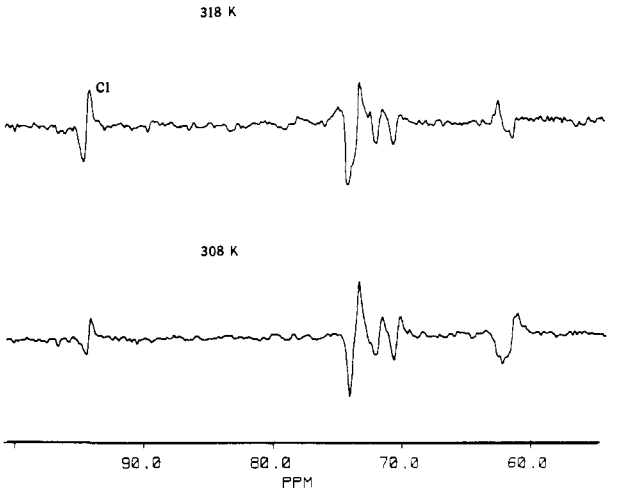

Figure 5. 125-MHz INEPT spectra of trehalose in CsPFO micelles showing temperature effects.

splitting is significantly smaller than 166 Hz, indicating a sizable negative contribution from dipolar coupling. There is, however, some uncertainty as to the magnitude of the dipolar coupling because it could be either smaller in magnitude than the J coupling or larger in magnitude than the J coupling and yield the same observed splitting. The former situation would yield a dipolar splitting of −120 Hz, while the latter would yield a splitting of −212 Hz. The correct magnitude can be determined by observing the splitting as the sample is carried to a higher ordered state. Ordering in the CsPFO liquid crystal increases inversely with temperature, producing a higher contribution of dipolar coupling at lower temperature. As Figure 5 indicates, the C1 splitting decreases from the higher to the lower temperature. The decrease in splitting indicates that the dipolar coupling is smaller than the J coupling; consequently, the C1–H1 dipolar contribution is assigned a value of −120 Hz. Due to the complexity of the ^{13}C NMR spectrum of other trehalose peaks in CsPFO, only the C1–H1 splitting will be used for orientational analysis.

The quadrupole and ^{13}C dipole information could conceivably define the orientation of the bonds in each glucose ring relative to the molecular director axis, and hence a molecular conformation as well as orientation. However, this would provide a rather indirect assessment of the primary conformational degrees of freedom, the angles θ and ψ about the glycosidic bond (ϕ and ψ are torsion angles H1–C1–O1–C1′ and C1–O1–C1′–H1′, respectively). It is evident from the structure of trehalose in Figure 1 that the internuclear distance between the anomeric protons would be a more direct probe of variation of ϕ and ψ angles. These protons are also relatively close to one another, offering the possibility of observing anomeric proton–anomeric proton dipolar interaction. The ^1H NMR spectrum of partially deuterated trehalose in CsPFO is presented in Figure 6. The spectrum in the region of anomeric protons at 5.3 ppm remains fairly simple; a benefit of their isolation from remaining molecular protons in the deuterated sample. By comparison of this spectrum to the spectrum observed in deuterium oxide solution (Figure 2), it is evident that the anomeric proton signal has been split into a doublet. There is little, if any, dipolar interaction between H1 and the deuterium at the H2 positions; hence the H1 proton doublet is attributed to an anomeric proton–anomeric proton dipolar interaction. The dipolar interactions between the H3, H5, and remaining H6, H6′ protons can be seen in the 3.5–4.5 ppm region. However, broad peaks render direct measurement of these dipolar splittings impossible. The anomeric ^1H dipolar coupling of 106 Hz completes the data set of the quadrupolar and dipolar interactions. These splittings are summarized in Table II.

Discussion

The search for a trehalose orientation and conformation consistent with experimental observations could take many forms. In the past, we have assumed a rigid sugar conformation and

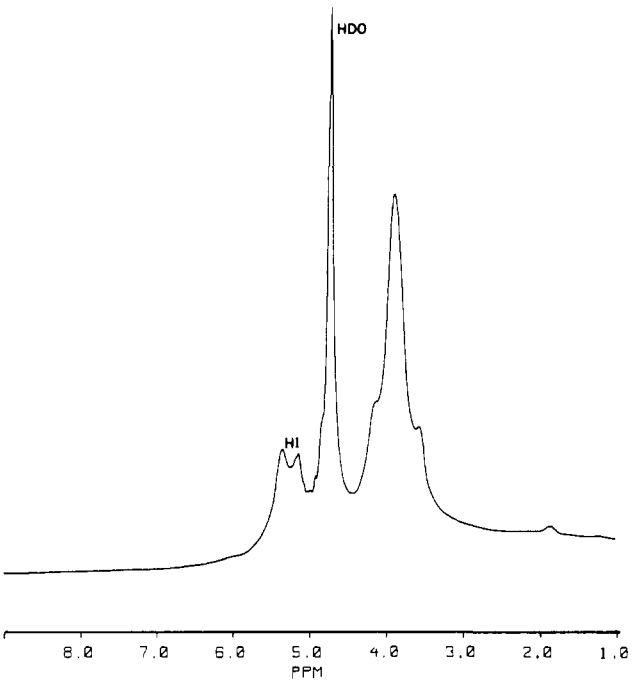

Figure 6. 500-MHz ^1H NMR spectrum of trehalose in CsPFO micelles.

Table II. Constraint Data

vector	interaction	splitting, Hz
H1–H1′	dipolar	106
C1–H1	dipolar	−120
C1′–H1′	dipolar	−120
C2–H2	quadrupolar	87
C2′–H2′	quadrupolar	87
C4–H4	quadrupolar	185
C4′–H4′	quadrupolar	185

Table III. Comparison of Geometries for Calculated Trehalose Structures (W = 20 kcal)

	conformer					
	A1		A2		B	
vector	init	final	init	final	initi	final
H1–H1′[a]	2.83	2.87	3.72	3.49	2.83	2.79
H1–H1′	79	77	61	54	86	90
C1–H1	60	61	54	51	143	134
C2–H2	128	126	119	125	120	124
C4–H4	126	127	112	124	123	123
C1′–H1′	121	119	126	129	127	133
C2′–H2′	46	54	61	54	121	124
C4′–H4′	47	53	65	56	116	122
ϕ_H	−50	−53	−88	−82	−50	−59
ψ_H	−49	−47	−88	−72	−49	−42

[a] Interproton distance in angstroms. All other values are angles, in degrees, relative to the director axis.

searched for an orientation that reproduces all observed splittings given a single adjustable order parameter.[5,6] This is similar to the approach used by Jarrel et al. for individual segments in glycolipids.[10,11] In the present case, we have data that we expect to be explicitly sensitive to conformation as well as orientation. We, therefore, prefer to follow an approach that allows adjustment of both orientation and conformation in the process of searching for a best fit to experimental observation.

Molecular mechanics and molecular dynamics programs allow for optimization of molecular conformation during the course of an energy minimization process. Normally the energy minimization involves only molecular potential energy functions, with terms that describe bond stretching, angular and dihedral distortions, electrostatic interactions, nonbonded interactions, and hydrogen-bonding interactions. However, the same algorithms that locate minima in these molecular functions can be used to

Table IV. Comparison of Experimental and Calculated Spectral Data

		conformer A1		conformer A2		conformer B	
vector	exptl	high W^a	low W^b	high W^a	low W^b	high W^a	low W^b
H1-H1′	±106	−107	−117	107	130	101	100
C1-H1	−120	−120	−120	−120	−120	−120	−120
C2-H2	±87	87	92	88	84	88	89
C4-H4	±185	185	185	185	185	185	185
C1′-H1′	−120	−120	−120	−120	−119	−120	−120
C2′-H2′	±87	89	91	−86	−77	88	96
C4′-H4′	±185	185	185	185	183	185	186
energy, kcal		−9.83	−11.10	−3.32	−10.36	−9.03	−11.11

[a] Minimizations run with 20-kcal weighting factor. [b] Minimizations run with 2-kcal weighting factor.

find minima in experimental error functions that minimize when the molecular geometry satisfies orientational or conformational constraints. It is clear that a search can be undertaken that simultaneously minimizes molecular and experimental functions.

We have presented suitable error functions for deuterium quadrupolar data and proton NOE distance constraints in the past.[23,24] In an analogous way, we can drive an error function that represents orientational information from dipolar data.

$$E_{\text{pseudo}} = W\left[\left\{\frac{\nu_{\text{calcd}}}{\nu_{\text{calcd}}^{\circ}}\right\}^2 - \left\{\frac{\nu_{\text{expt}}}{\nu_{\text{expt}}^{\circ}}\right\}^2\right]^2 \quad (3)$$

To avoid assuming an order parameter, we use one of the experimental splittings as a scaling factor, $\nu_{\text{expt}}^{\circ}$. ν_{calcd} is the dipolar splitting, (as given in eq 2), calculated for the current molecular conformation and ν_{expt} represents the corresponding experimental splitting. W is a weighting parameter that is chosen to adjust the pseudoenergy contribution to be similar in magnitude to the other energy contributions. The generalized form in eq 3 can be used to represent quadrupolar data as well if eq 1 rather than eq 2 is used for ν_{calcd}. These additional terms were added to the force field of the molecular modeling package AMBER.[19,20]

One term of the above form should be included for each of the experimental parameters that can be measured. In principle, there are four deuterium quadrupolar splittings, two $^{13}C-^{1}H$ and one $^{1}H-^{1}H$ dipolar splitting. In practice, only one splitting is measured for a symmetry-related pair, i.e., H4 and H4′. This equivalence could arise for two different reasons. One is that the trehalose molecule is oriented so as to maintain this equivalence. The other is that rapid 180° flips about the twofold symmetry axis lead to averaging to equivalent splittings for the symmetry-related pairs. The latter model is motionally more complex and therefore we will confine our studies to a search for a configuration in which symmetry-related sites have identical instantaneous splittings.

Another problem in fitting data is the tendency for molecular mechanics minimization schemes to converge to the closest local minimum instead of finding the global minimum energy conformation. Our solution to this problem is to globally search for approximate orientational solutions and then refine our search beginning with the several possible director axes identified by this search. A grid search for director orientations that satisfy the experimental splittings was performed with an idealized structure close to that of the crystal structures.[25,26] When generous bounds were set, at about twice the typical experimental line width, this procedure generated three possible directors. Beginning with the molecule in each of these three possible orientations, we allowed the combined theoretical and experimental AMBER potential energy function to adjust the orientation and conformation to optimize fit to experimental data.

The search over conformational space was extended by altering the conformations of starting structures with six distinct sets of glycosidic torsions, ϕ, ψ, and using the new conformations with each of the three director orientations. The sets of torsions used were (−50, −50), (−60, −60), (−90, −90), (180, 180), (90, 90), and (60, 60). Preliminary minimizations with a truncated potential energy function containing the pseudoenergy term and only bonding and angular energy terms to simplify the potential energy surface and allow some expansion of the convergence radius were performed. This was followed by minimizations where all the energy terms and the pseudoenergy terms were present, with the pseudo potential weighting factor, W, set at 20 kcal. Under these conditions, the molecular mechanics program is able to produce torsional changes as large as 30° and structures dramatically different from initial conformations.

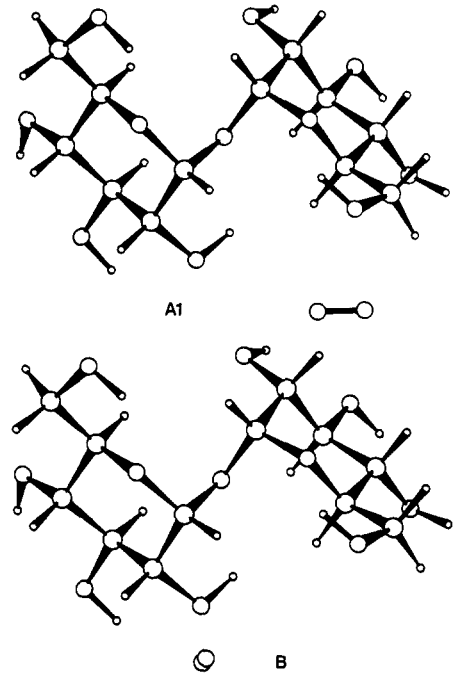

Figure 7. Orientation of trehalose in CsPFO micelles. (A) Structure A1, (B) structure B. The vector at the bottom shows the field direction in each case.

Only a small number of starting structures converge to acceptable agreement with experimental data. Of the three director orientations, one consistently resulted in solutions that were energetically higher than the solutions from the other two orientations (A and B). This director orientation will not be considered any further. Of the structures with orientation A, only two geometries fit experimental data to within one-quarter of a typical line width and had reasonable molecular energies (Table III). The structure A2, which differs by not more than 12° from A1, is 6 kcal higher in energy and probably does not represent the major conformation. In the case of orientation B, there was only one final structure that satisfied the above criteria. Two starting structures that differed initially by 10° in ϕ_H and ψ_H both converged to this conformation (B).

Reducing the weighting factor, W, by an order of magnitude, to a point where molecular energetics dominate the calculations,

(23) Ram, P.; Prestegard, J. H. *J. Am. Chem. Soc.* **1988**, *110*, 2383–2388.
(24) Scarsdale, J. N.; Ram, P.; Prestegard, J. H.; Yu, R. K. *J. Comput. Chem.* **1988**, *9*, 133–147.
(25) Brown, G. M.; Rohrer, D. C.; Berking, B.; Beevers, C. A.; Gould, R. O.; Simpson, R. *Acta Crystallogr.* **1972**, *B28*, 3145–3158.
(26) Taga, T.; Senma, M.; Osaki, K. *Acta Crystallogr.* **1972**, *B28*, 3258–3263.

changes the energies and the agreement to experimental data for A1 and B by 1.5 kcal in energy and 10 Hz or less in the H1-H1′ dipolar splitting. The other splittings for A1 and B change by less than 8 Hz (Table IV). These changes are well within experimental error. Structure A2 relaxes to a structure that is energetically more favorable by 6 kcal but violates the H1-H1′ constraint by more than 20 Hz and the C2-H2 constraint by 9 Hz. Structure A2 can therefore be regarded as less probable based on either higher molecular energies or unacceptable deviations from experiment.

We believe procedures used in searching for preferred structures are reasonably robust. Initial searches for director axes with an assumed fixed conformation employ the same grid search algorithms used in the past.[5,6,10-12] The addition of molecular mechanics based minimization allows a moderately efficient extension of the search to cases in which conformational changes may have occurred. The fact that we see cases of displaced starting structures return to a common point suggests that we are approaching an adequate range of conformational search. The inclusion of a molecular mechanics minimization is also advantageous in cases where experimental data are too sparse to independently define a conformation. The molecular force field adds, in a systematic way, bonding constraints that are often implicit in choosing one conformation from experimental observations that give multiple solutions.[10-12,23]

Despite the increased data available from both deuterium and dipolar information, and the use of molecular mechanics constraints of allowed conformations, we are unable to distinguish structure A1 and B and define a single director orientation for trehalose. Energies for orientations A1 and B differ by less than 1 kcal with either high or low weights. All the experimental splittings are satisfied to within 0.25 of a typical line width even at low weights. It is interesting, however, that both the structures A1 and B1 have the same molecular conformation. Of all the geometries studied for each orientation only one geometry can satisfy the experimental constraints, and this geometry is nearly identical for both orientations A1 and B. Low-weight ϕ_H and ψ_Hs correspond to −61, −41 and −58, −44, respectively, while the internuclear distances, H1-H1′ are 2.9 and 2.8 Å, respectively. The two structures are shown in Figure 7. These are in agreement with the solution structure.[21] Deviations from the values seen in the two crystal structures are small, less than 5° in ϕ_H and 12° in ψ_H.[25,26] As suggested in our initial analysis of quadrupolar splittings, θs for the deuterium-labeled sites are close to 54 or 126°, causing the relatively small splittings. Order parameters of 0.02 are similar to those observed previously for sucrose and mannose.[4,5]

Acknowledgment. This research was supported by grants from the National Institutes of Health (GM 33225), and benefited from instrumentation provided through the shared instrumentation program of the Division of Research Resources of the National Institutes of Health (RR 02379).

Registry No. CsPFO, 17125-60-9; trehalose, 99-20-7.

Sulfur K-Edge X-ray Absorption Spectroscopy of Petroleum Asphaltenes and Model Compounds

Graham N. George and Martin L. Gorbaty*

Contribution from the Corporate Research Laboratories, Exxon Research and Engineering Company, Annandale, New Jersey 08801. *Received July 21, 1988*

Abstract: The utility of sulfur K-edge X-ray absorption spectroscopy for the determination and quantification of sulfur forms in petroleum asphaltenes has been investigated. Both X-ray absorption near edge structure (XANES) and extended X-ray absorption fine structure (EXAFS) spectra were obtained for a selected group of model compounds and for several petroleum asphaltene samples. For the model compounds the sulfur XANES was found to vary widely from compound to compound and to provide a fingerprint for the form of sulfur involved. The use of third derivatives of the spectra enabled discrimination of mixtures of sulfidic and thiophenic model compounds and allowed approximate quantification of the amount of each component in the mixtures and in the asphaltene samples. These results represent the first demonstration that nonvolatile sulfur forms can be distinguished and approximately quantified by direct measurement.

A major gap in our current knowledge of the chemistry of heavy hydrocarbons and coal concerns the chemical forms and quantities of organically bound sulfur in these materials. At best, current knowledge is qualitative and is based almost entirely upon characterization of volatile products. For coals, total organic sulfur is quantified by the difference between total and pyritic sulfur analyses. The different forms of sulfur have been assigned by a variety of methods, including mass spectroscopy of extractable materials and of liquid products, methyl iodide derivitization, catalytic decomposition, and oxidative techniques.[1] More recently, methods have been reported using a two-step chemical modification in conjunction with ^{13}C NMR spectroscopy to determine the chemical forms of sulfur in nonvolatile petroleum materials.[2] However, to date, no available method is completely adequate for directly determining both the forms and the amounts of organically bound sulfur in native coals and petroleum materials.

This report investigates the applications of X-ray absorption spectroscopy for the purpose of speciating and quantifying the forms of organic sulfur in solids and nonvolatile liquids. In earlier work Hussain et al.,[3] Spiro et al.,[4] and, later, Huffman et al.[5,6] demonstrated the potential of sulfur X-ray absorption spectroscopy in the qualitative determination of sulfur forms in coals; however, they made no attempt at quantification. Sulfur K-edge X-ray

(1) Van Krevelen, D. W. *Coal*; Elsevier: Amsterdam, 1961; p 171.
(2) Rose, K. D.; Francisco, M. A. *J. Am. Chem. Soc.* **1988**, *110*, 637.
(3) Hussain, Z.; Umbach, E.; Shirley, D. A.; Stohr, J.; Feldhaus, J. *Nucl. Instrum. Methods* **1982**, *195*, 115.
(4) Spiro, C. L.; Wong, J.; Lytle, F. W.; Greegor, R. B.; Maylotte, D. H.; Lamson, S. H. *Science* **1984**, *226*, 48.
(5) Huffman, G. P.; Huggins, F. E.; Shah, N.; Bhattacharyya, D.; Pugmire, R. J.; Davis, B.; Lytle, F. W.; Greegor, R. B. In *Processing and Utilization of High Sulfur Coals II*; Chugh, Y. P., Caudle, R. D., Eds.; Elsevier: Amsterdam, 1987; p 3.
(6) Huffman, G. P.; Huggins, F. E.; Shah, N.; Bhattacharyya, D.; Pugmire, R. J.; Davis, B.; Lytle, F. W.; Greegor, R. B. *ACS Div. Fuel Chem. Prep.* **1988**, *33*, 200.

0002-7863/89/1511-3182$01.50/0